



X-rays from HH210 in the Orion nebula

Nicolas Grosso, Eric D. Feigelson, Konstantin V. Getman, Joel Kastner, John Bally, Mark J. McCaughrean

► To cite this version:

Nicolas Grosso, Eric D. Feigelson, Konstantin V. Getman, Joel Kastner, John Bally, et al.. X-rays from HH210 in the Orion nebula. *Astronomy and Astrophysics - A&A*, 2006, 448, pp.29-32. 10.1051/0004-6361:200600004 . hal-00017504

HAL Id: hal-00017504

<https://hal.science/hal-00017504>

Submitted on 23 Jan 2006

HAL is a multi-disciplinary open access archive for the deposit and dissemination of scientific research documents, whether they are published or not. The documents may come from teaching and research institutions in France or abroad, or from public or private research centers.

L'archive ouverte pluridisciplinaire **HAL**, est destinée au dépôt et à la diffusion de documents scientifiques de niveau recherche, publiés ou non, émanant des établissements d'enseignement et de recherche français ou étrangers, des laboratoires publics ou privés.

X-rays from HH 210 in the Orion Nebula

N. Grosso¹, E. D. Feigelson², K. V. Getman², J. H. Kastner³, J. Bally⁴, and M. J. McCaughrean^{5,6}

¹ Laboratoire d'Astrophysique de Grenoble, Université Joseph-Fourier, F-38041 Grenoble cedex 9, France
e-mail: Nicolas.Grosso@obs.ujf-grenoble.fr

² Department of Astronomy and Astrophysics, Pennsylvania State University, University Park, PA 16802, USA

³ Center for Imaging Science, Rochester Institute of Technology, Rochester, New York 14623-5604, USA

⁴ Center for Astrophysics and Space Astronomy, University of Colorado at Boulder, CB 389, Boulder, CO 80309, USA

⁵ School of Physics, University of Exeter, Stocker Road, Exeter EX4 4QL, Devon, UK

⁶ Astrophysikalisches Institut Potsdam, An der Sternwarte 16, D-14482 Potsdam, Germany

Abstract. We report the detection during the *Chandra Orion Ultradeep Project* (COUP) of two soft, constant, and faint X-ray sources associated with the Herbig-Haro object HH 210. HH 210 is located at the tip of the NNE finger of the emission line system bursting out of the BN-KL complex, northwest of the Trapezium cluster in the OMC-1 molecular cloud. Using a recent H α image obtained with the ACS imager on board *HST*, and taking into account the known proper motions of HH 210 emission knots, we show that the position of the brightest X-ray source, COUP 703, coincides with the emission knot 154-040a of HH 210, which is the emission knot of HH 210 having the highest tangential velocity (425 km s⁻¹). The second X-ray source, COUP 704, is located on the complicated emission tail of HH 210 close to an emission line filament and has no obvious optical/infrared counterpart. Spectral fitting indicates for both sources a plasma temperature of ~ 0.8 MK and absorption-corrected X-ray luminosities of about 10^{30} erg s⁻¹ (0.5–2.0 keV). These X-ray sources are well explained by a model invoking a fast-moving, radiative bow shock in a neutral medium with a density of ~ 12000 cm⁻³. The X-ray detection of COUP 704 therefore reveals, in the complicated HH 210 region, an energetic shock not yet identified at other wavelengths.

Key words. ISM: Herbig-Haro objects – ISM: individual objects: HH 210 – X-rays: ISM

1. Introduction

Outflow activity is ubiquitous in young stellar objects (YSO), and intimately connected to the accretion process building up the mass of stars. The interaction of outflow from YSO and the interstellar medium produces bow shocks associated with optically luminous small nebulae, called Herbig-Haro (HH) objects (Herbig 1950; Haro 1952; see review by Reipurth & Bally 2001). Optical emission from HH objects includes Hydrogen Balmer lines, [O I], [S II], [N II], [O III], tracing plasma with temperatures of several 10^3 to 10^5 K. During these last years a handful of HH objects have been detected in X-rays, tracing plasma with temperatures of a few 10^6 K, as expected from the high velocities of these shocks (e.g., Raga et al. 2002). The emission knot H of HH 2 was the first detected in X-rays; it also exhibits strong H α and free-free radio continuum emission (Pravdo et al. 2001). HH 80 and HH 81 are excited by a massive protostar, and are among the most luminous HH objects in the optical; emission knots A and G/H of HH 80, and emission knot A of HH 81 are now the most luminous known in X-rays (Pravdo et al. 2004).

The soft X-ray emission from L1551 IRS5, associated with HH 154 by Favata et al. (2002), is now considered as arising from a shock at the base of the jet of this protostar binary (Bally et al. 2003; Bonito et al. 2004). Recently, soft X-ray

excesses were found in the X-ray spectra of the ‘Beehive’ proplyd (Kastner et al. 2005) and DG Tau (Güdel et al. 2005), two YSOs with jets. Remarkably, in both sources, this soft and constant X-ray emission suffers less extinction than the harder and variable X-ray component likely emitted by the stellar corona, suggesting that it comes from shocks along the base of these jets.

In January 2003, the *Chandra Orion Ultradeep Project* (COUP) was carried out with ACIS-I (Garmire et al. 2003) on board the *Chandra* X-ray Observatory (Weisskopf et al. 2002). COUP consisted of a nearly continuous exposure over 13.2 days centered on the Trapezium cluster in the Orion Nebula, yielding a total on-source exposure time of 838 ks, i.e. 9.7 days (Getman et al. 2005b). Among the 1616 COUP X-ray sources, there are only about fifty X-ray sources with the median energy of their X-ray photons lower than 1 keV, i.e. having a very soft X-ray spectrum. The bulk of this soft X-ray source sample is associated with optical/infrared stars; two sources may be spurious; and two other sources without counterparts may be newly discovered very low mass members of the Orion nebula cluster. Of the very soft sources, only COUP 703 and COUP 704 are possibly associated with an HH object, HH 210 (Getman et al. 2005a; Kastner et al. 2005). More generally

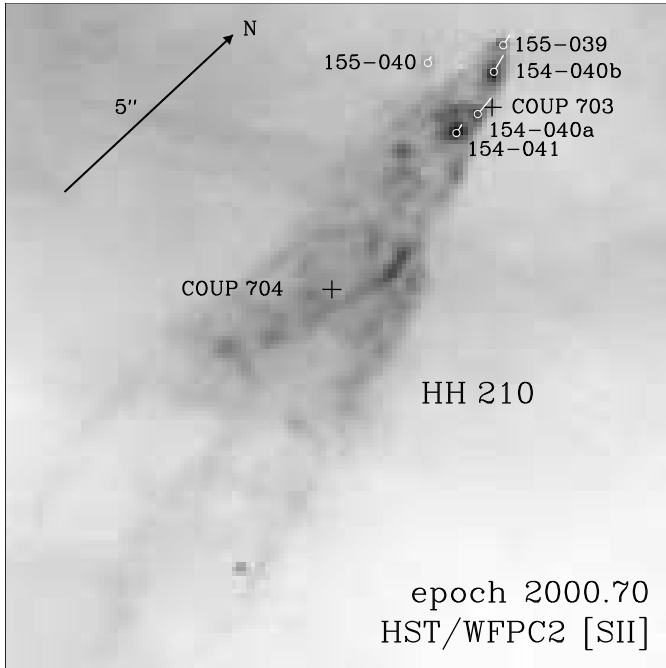


Fig. 1. *HST*/WFPC2 image of HH 210 for epoch 2000.70 in [S II] (adapted from Fig. 2 of Doi et al. 2002). Each pixel is $0''.1$ on a side, the color stretch is linear. HH 210 shows a typical bow shock structure containing numerous emission knots and filaments. The two crosses mark epoch 2003.04 positions of COUP 703 and COUP 704 (Getman et al. 2005b); cross sizes indicate the total positional uncertainties of these X-ray sources ($0''.14$). The white arrows indicate velocity and epoch 2003.04 position for emission knots with proper-motion measured in [S II] by Doi et al. (2002). The white $0''.08$ -radius circles indicate the optical resolution of *HST*.

there is in COUP no other X-ray source associated with HH objects (Getman et al. 2005a).

HH 210 is located $2.7'$ -north of θ^1 Ori C in the OMC-1 molecular cloud, and is one of the brightest HH objects in this area revealed by emission of [O I] (Axon & Taylor 1984; Taylor et al. 1986). It belongs to the powerful CO outflow from the BN-KL region, which produces a spectacular set of H_2 bow shocks and trailed wakes; it is located at the tip of the NNE finger which is one of the brightest emission systems in [Fe II] and lacks a trailed H_2 wake (Allen & Burton 1993). HH 210 has a pronounced bow shape containing numerous knots and complicated filaments in [S II] (see Fig. 1).

We present in Sect. 2 the astrometry and spectral analysis of the X-ray sources associated with HH 210; we discuss in Sect. 3 the origin of these X-ray emissions.

2. Astrometry and spectral analysis of the X-ray sources associated with HH 210

We used the COUP source catalog and data products of Getman et al. (2005b). A detailed discussion of the COUP data, encompassing source detection, photon extraction, spectral analysis, and variability analysis can be found in Getman et al. (2005b).

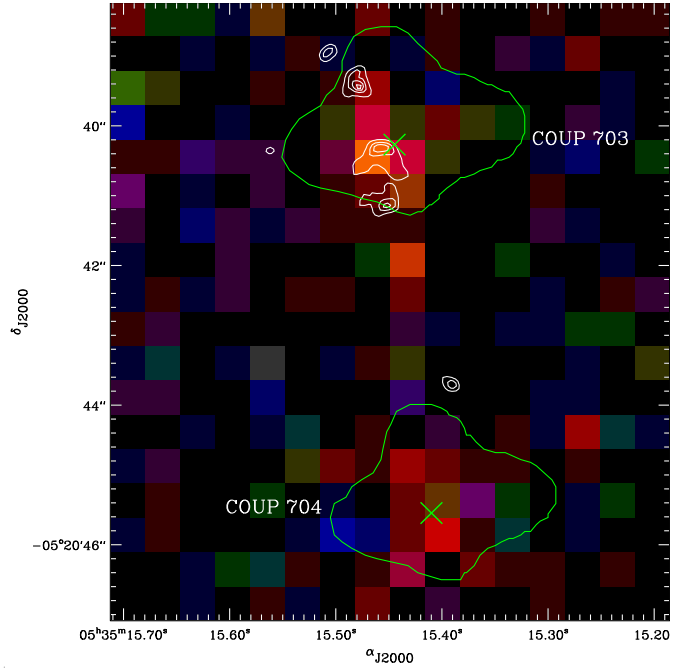


Fig. 2. COUP view of HH 210. Red, green, and blue represent photons in the 0.5–1.7 keV, 1.7–2.8 keV, and 2.8–8.0 keV energy bands, respectively (Lupton et al. 2004). Green crosses and contours mark the centre of COUP sources and source extraction polygons ($\sim 87\%$ encircled energy using PSF at 1.5 keV). Cross sizes indicate the total positional uncertainties of these X-ray sources ($0''.15$). White contours show $H\alpha + [N II]$ knots observed with *HST*/ACS ($0''.05$ -pixels on a side; epoch 2004.05, Bally et al. 2005), which were moved individually to epoch 2003.04 using proper-motions of Doi et al. (2002). COUP 703 coincides with 154-040a HH 210, the emission knot having the highest tangential velocity (425 km s^{-1} ; see Fig. 1).

We use *HST* archival images to compare the position of COUP sources with emission knots of HH 210.

The best view of the HH 210 emission system is obtained in the optical using [S II] doublet ($\lambda 6717 + \lambda 6731$ lines) or [O I] ($\lambda 6300$ line), where both bow shocks and a complicated emission tail are visible, whereas in $H\alpha$ only the heads of the bow shocks are visible. Figure 1 shows the HH 210 emission system at epoch 2000.70 obtained with the WFPC2 on board *HST* with F673N filter, selecting [S II] (program GO8121NW; Doi et al. 2002). The HH 210 emission system in the [O I] line is very similar. We extracted star positions in the full field-of-view of *HST*/WFPC2 using *Source Extractor* (version 2.3.2; Bertin & Arnouts 1996)¹, and cross-correlated these with COUP positions. The estimated residual registration error between fifteen stars in the WFPC2 image and the corresponding COUP sources is $0''.08$. Finally, the total positional accuracy of X-ray sources, which has a positional uncertainty in COUP of $0''.12$, is $0''.14$ in Fig. 1. From this WFPC2 image and a previous one obtained five years before, Doi et al. (2002) measured the proper-motion of several [S II] knots of HH 210, ranging from 153 km s^{-1} for 155-040 HH 210 to 425 km s^{-1} for 154-

¹ Available at <http://terapix.iap.fr>.

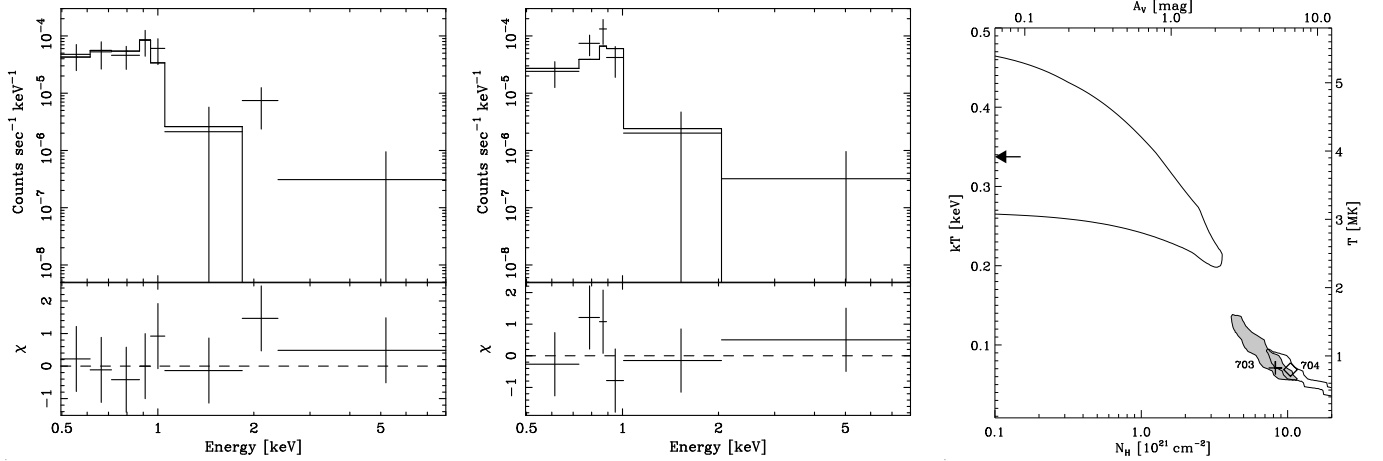


Fig. 3. X-ray spectra of COUP 703 (left) and COUP 704 (middle), and confidence regions of the plasma parameters (right). Each spectral bin contains at least 5 events. We used for the spectral fitting a collisionally-ionized plasma model (APEC), assuming a plasma with solar elemental abundance (Anders & Grevesse 1989), with X-ray absorption model (WABS; Morrison & McCammon 1983). Fit parameters are given in Table 1. In the right panel, the grey region indicates for COUP 703 the confidence regions at the 68% level of the plasma temperature and the absorption. The plus sign and diamond mark the best parameter values for COUP 703 and COUP 704 (high N_H /low kT solution), respectively. The arrow indicates the high temperature value for the null absorption solution of COUP 704.

Table 1. Spectral parameters of X-ray sources associated with HH 210 using a WABS×APEC plasma model with solar elemental abundance. We used Chi statistics with standard weighting. Confidence ranges at the 68% level ($\Delta\chi^2 = 1$; corresponding to $\sigma = 1$ for Gaussian statistics) are given in parentheses. Q in Col. (8) is the probability that the best-fit model matches the data, given the value of χ^2 and ν , the degree of freedom in Col. (7). The emission measure in Col. (6) and the logarithm of the X-ray luminosities in the 0.5–2 keV energy range observed/corrected for absorption in Col. (9) were computed assuming a distance of 450 pc.

COUP	CXOONCJ	Net	N_H	kT	EM	χ^2_ν (ν)	Q	$\log L_S / \log L_{S,c}$
#		conts	10^{21} cm^{-2}	keV	10^{55} cm^{-3}		%	erg s^{-1}
(1)	(2)	(3)	(4)	(5)	(6)	(7)	(8)	(9)
703	053515.4-052040.3	31	8 (5–11)	0.07 (0.05–0.14)	1.5	0.70 (5)	62	27.3 / 30.0
704	053515.4-052045.5	24	0 (≤ 0.3)	0.33 (0.22–0.45)	3×10^{-5}	1.08 (3)	36	27.1 / 27.1
			10 (7–13)	0.07 (≤ 0.09)	48	1.20 (3)	31	27.1 / 30.3

040a HH 210. Using these proper motions we plotted in Fig. 1 white arrows pointing at the estimated position of HH 210 knots for COUP epoch 2003.04. We conclude that the position of COUP 703 is consistent with the position of the [S II] knot 154-040a HH 210, whereas COUP 704 is located on the complicated emission tail of HH 210 close to an emission filament.

The image of HH 210 obtained with ACS on board *HST* at epoch 2004.05 by Bally et al. (2005) is the closest in time to COUP. This ACS observation was made in F658N filter selecting H α ($\lambda 6563$ line) and [N II] ($\lambda 6584$ line), and hence detected mainly the heads of the bow shocks (Bally et al. 2005). To register this ACS image with COUP, we extracted position of ACS stars, and cross-correlated these with COUP positions. The estimated residual registration error between about ninety ACS stars and their corresponding COUP sources is $0''.12$. Finally, the total positional accuracy between X-ray sources, which has a positional uncertainty in COUP of $0''.1$, and ACS sources is $0''.15$. Figure 2 shows the COUP image of HH 210 using X-ray colors. The contour map indicates the brightest emission knots observed in H α with *HST*/ACS, which were moved individually to match epoch 2003.04 using proper-motions of

Doi et al. (2002). The most southern H α knot has no known proper-motion; therefore we conservatively assumed for this knot the largest proper-motion of HH 210 knots. We conclude that COUP 703 coincides with the emission knot with the highest tangential velocity (425 km s^{-1}), 154-040a HH 210. In contrast, COUP 704 is not associated with any bright H α emission knot, or point source in the *VLT J*-, *H*-, *K_S*-band survey (McCaughrean et al., in preparation) and the *IRTF L*-band survey (McCaughrean et al. 1996). We note that it is located near a filament of [S II] emission (see Fig. 1).

We compared the spatial distribution of events in COUP 703 and 704 with those in the X-ray counterpart of a nearby star, after adding to this reference source uniformly distributed background events to match the background level measured in the extraction regions of COUP 703 and 704. Kolmogorov-Smirnov test shows that COUP 703 and 704 are compatible with unresolved sources. Therefore the angular resolution of *Chandra* at $2.7'$ off-axis, i.e. $\sim 1''$, is an upper limit for the size of these objects.

The observed X-ray spectra are shown in Fig. 3. In XSPEC (version 11.3), we used for the spectral fitting between 0.5

and 8 keV (corresponding to channels PI=35–548) a photoelectric absorption (WABS) combined with a collisionally-ionized plasma model (APEC), which provides plasma temperatures down to 0.1 MK. Table 1 gives our best fit parameters. For the source with the highest net counts, COUP 703, we found a column density of absorbing material of $N_{\text{H},21} \approx 8 \text{ cm}^{-2}$ (5–11 cm^{-2}), equivalent to $A_V \sim 5 \text{ mag}$ (3–7 mag) (Vuong et al. 2003), and a plasma temperature of $T \approx 0.8 \text{ MK}$ (0.5–1.6 MK). For COUP 704, the absolute χ^2 minimum corresponds to null absorption and high plasma temperature, with a low intrinsic X-ray luminosity (see the right panel of Fig. 3). This combination of high plasma temperature and low X-ray luminosity would imply a small radius ($\sim 10^{14} \text{ cm}$) of the object driving the shock (see Sect. 3). However, another solution with a similar goodness-of-fit exists with higher absorption and lower plasma temperature, similar to the best-fit plasma parameters found for COUP 703. The latter parameters therefore likely represent a better approximation of the actual physical conditions in the plasma giving rise to COUP 704. The absorption-corrected X-ray luminosities of COUP 703 and 704 implied by the spectral fitting are about $10^{30} \text{ erg s}^{-1}$ (0.5–2.0 keV).

3. Discussion

HH 210 displays the largest proper motion among the outflow fingers extending away from BN-KL, moreover the line emission is blue-shifted, suggesting a deprojected velocity of about 500 km s^{-1} (Axon & Taylor 1984; Taylor et al. 1986; Hu 1996). 154-040a HH 210 is also the brightest feature in [O III] and has a small bow shock attached to it (O’de’l et al. 1997; Doi et al. 2002). The tip of the bow shock is seen as a knot in [N II], H α , [O III]; hence the tip is the fastest moving portion of the shock. However, the fact that the [O III] emission requires only a shock with a speed of about 90 km s^{-1} and that the [O III] emission is seen only at the tip of the bow, indicates that this HH object is moving in the wake of other shocks moving ahead of it (Doi et al. 2002).

The observed X-ray emission can be explained with fast moving bow shocks. The postshock temperature in the adiabatic (non-radiative) portion of a shock is given by $T_{\text{ps}}/\text{K} = 2.9 \times 10^5 / (1+X) \times V_{100}^2$ (Ostriker & McKee 1988), where V_{100} is the velocity of the shock front with respect to the downstream material (the shock velocity) in units of 100 km s^{-1} and X is the ionization fraction of the preshock gas ($X=0$ for a neutral medium and 1 for a fully ionized one). Thus, COUP 703 and COUP 704 plasma temperatures of $\sim 0.8 \text{ MK}$ require a shock speed of $\sim 170 \text{ km s}^{-1}$ for a shock moving into a mostly neutral medium, or $\sim 240 \text{ km s}^{-1}$ for a shock moving into a fully ionized medium. The lower speed is comparable with the bow shock velocity of 133 km s^{-1} estimated by O’de’l et al. (1997) from the deprojected velocity and the opening angle of the bow wing.

The expected X-ray luminosity of a shock-heated source depends on the emissivity per unit volume, which depends on the plasma temperature and density, the volume of the emitting region, and the type of shock, radiative or non-radiative (Raga et al. 2002). Neglecting the line emission, Raga et al. (2002) find for a radiative shock $L_{\text{r}}/\text{erg s}^{-1} = 1.64 \times$

$10^{28} n_{100} r_{\text{b},16}^2 V_{100}^{5.5}$; and for a non-radiative shock $L_{\text{nr}}/\text{erg s}^{-1} = 1.8 \times 10^{29} n_{100}^2 r_{\text{b},16}^3 V_{100}$, where n_{100} is the preshock density in units of 100 cm^{-3} and $r_{\text{b},16}$ is the radius of the object driving the shock in units of 10^{16} cm . The X-ray luminosity of a bow shock is the minimum of these two values. The multiplicative factor to take into account line emission is 2.5 and 3.0 at 0.1 MK and 1 MK, respectively (Raga et al. 2002). The *HST/ACS* observation of 154-040a HH 210 shows a radius of $0''.15$ (Fig. 2), or about 10^{15} cm at a distance of 450 pc. Using this dimension for the X-ray source, a shock speed of 170 km s^{-1} , and a preshock density of about 12000 cm^{-3} , we find $L_{\text{r}} \sim 3.3 \times 10^{29} \text{ erg s}^{-1}$. Thus taking into account line emission, a bow shock flow can readily explain the X-ray luminosities observed from COUP 703 and COUP 704. citetallen93 found a similar density of $\sim 10^4 \text{ cm}^{-3}$ for the electronic density inferred from the [Fe II] spectra of the emission knots. The location of HH 210 inside OMC-1 but close to the limit of the H II region may explain this density and why the medium is not yet fully ionized by the radiation field of the Trapezium cluster.

We conclude that COUP 703 is the counterpart of the emission knot 154-040a of HH 210, and its X-ray emission can be explained by a radiative bow shock. The X-ray emission of COUP 704 can also be explained by a fast-moving, radiative shock toward the tail of HH 210. Optical/infrared observations are still needed at other epochs to reveal in the complicated HH 210 region the proper motion of the counterpart to this X-ray source.

Acknowledgements. We thanks an anonymous referee for useful comments which improved the paper. COUP is supported by the *Chandra* Guest Observer grant SAO GO3-4009A (E. Feigelson, PI). Further support was provided by the *Chandra* ACIS Team contract SV4-74018.

References

- Allen, D. A. & Burton, M. G. 1993, *Nature*, 363, 54
- Anders, E. & Grevesse, N. 1989, *Geochim. Cosmochim. Acta*, 53, 197
- Axon, D. J. & Taylor, K. 1984, *MNRAS*, 207, 241
- Bally, J., Feigelson, E., & Reipurth, B. 2003, *ApJ*, 584, 843
- Bally, J., Licht, D., Smith, N., & Walawender, J. 2005, *AJ*, 129, 355
- Bertin, E. & Arnouts, S. 1996, *A&AS*, 117, 393
- Bonito, R., Orlando, S., Peres, G., Favata, F., & Rosner, R. 2004, *A&A*, 424, L1
- Doi, T., O’De’l, C. R., & Hartigan, P. 2002, *AJ*, 124, 445
- Favata, F., Fridlund, C. V. M., Micela, G., Sciortino, S., & Kaas, A. A. 2002, *A&A*, 386, 204
- Güdel, M., Skinner, S. L., Briggs, K. R., et al. 2005, *ApJ*, 626, L53
- Garmire, G. P., Bautz, M. W., Ford, P. G., Nousek, J. A., & Ricker, G. R. 2003, in *X-Ray and Gamma-Ray Telescopes and Instruments for Astronomy*, J. E. Truemper, H. D. Tananbaum (eds.), *Proceedings of the SPIE*, vol. 4851, p. 28–44
- Getman, K. V., Feigelson, E. D., Grosso, N., et al. 2005a, *ApJS*, 160, 353

- Getman, K. V., Flaccomio, E., Broos, P. S., et al. 2005b, *ApJS*, 160, 319
- Haro, G. 1952, *ApJ*, 115, 572
- Herbig, G. H. 1950, *ApJ*, 111, 11
- Hu, X. 1996, *AJ*, 112, 2712
- Kastner, J. H., Franz, G., Grosso, N., et al. 2005, *ApJS*, 160, 511
- Lupton, R., Blanton, M. R., Fekete, G., et al. 2004, *PASP*, 116, 133
- McCaughrean, M. J., Rayner, J., Zinnecker, H., & Stauffer, J. 1996, *Lecture Notes in Physics: Disks and Outflows Around Young Stars*, 465, 33
- Morrison, R. & McCammon, D. 1983, *ApJ*, 270, 119
- O'dell, C. R., Hartigan, P., Lane, W. M., et al. 1997, *AJ*, 114, 730
- Ostriker, J. P. & McKee, C. F. 1988, *Reviews of Modern Physics*, 60, 1
- Pravdo, S. H., Feigelson, E. D., Garmire, G., et al. 2001, *Nature*, 413, 708
- Pravdo, S. H., Tsuboi, Y., & Maeda, Y. 2004, *ApJ*, 605, 259
- Raga, A. C., Noriega-Crespo, A., & Velázquez, P. F. 2002, *ApJ*, 576, L149
- Reipurth, B. & Bally, J. 2001, *ARA&A*, 39, 403
- Taylor, K., Dyson, J. E., Axon, D. J., & Hughes, S. 1986, *MNRAS*, 221, 155
- Vuong, M. H., Montmerle, T., Grosso, N., et al. 2003, *A&A*, 408, 581
- Weisskopf, M. C., Brinkman, B., Canizares, C., et al. 2002, *PASP*, 114, 1